ORGANISMAL BIOLOGY

Prepatterning of *Papilio xuthus* caterpillar camouflage is controlled by three homeobox genes: *clawless*, *abdominal-A*, and *Abdominal-B*

H. Jin, T. Seki, J. Yamaguchi, H. Fujiwara*

Color patterns often function as camouflage to protect insects from predators. In most swallowtail butterflies, younger larvae mimic bird droppings but change their pattern to mimic their host plants during their final molt. This pattern change is determined during the early fourth instar by juvenile hormone (JH-sensitive period), but it remains unclear how the prepatterning process is controlled. Using *Papilio xuthus* larvae, we performed transcriptome comparisons to identify three camouflage pattern–associated homeobox genes [*clawless*, *abdominal-A*, and *Abdominal-B* (*Abd-B*)] that are up-regulated during the JH-sensitive period in a region-specific manner. Electroporation-mediated knockdown of each gene at the third instar caused loss or change of original fifth instar patterns, but not the fourth instar mimetic pattern, and knockdown of *Abd-B* after the JH-sensitive period had no effect on fifth instar patterns. These results indicate the role of these genes during the JH-sensitive period and in the control of the prepatterning gene network.

INTRODUCTION

Body coloration is an adaptive and ecologically important trait that is often involved in prey-predator interactions and diversified among closely related species. In insects, in particular, mimesis (mimicry), crypsis (camouflage), and aposematism (warning signals) are successful survival strategies to effectively deceive or avoid predators (*1*–*3*). Recent studies on butterfly wings have unveiled the gene regulation and molecular mechanisms controlling color pattern formation involved in Müllerian or Batesian mimicry (*4*–*10*). However, our understanding of color pattern formation in caterpillars remains limited, although larvae are soft-bodied and much more immobilized on the host plant than butterflies, making them an easy prey for birds once they have been noticed.

Most species in the *Papilio* genus drastically change their body coloration patterns during larval development (*11*, *12*), and these changes are fixed and irreversible (*13*). For example, in *Papilio xuthus* (Asian swallowtail butterfly), younger larvae from the first to the fourth instar show black and brown color patterns with white V-shaped patches, which is thought to mimic bird droppings (mimetic pattern) (Fig. 1A). In the final instar, however, they switch their coloration pattern to a greenish body with a pair of false eyespots on the third thoracic segment (T3) and a dark green, V-shaped marking on the dorsal side of the abdominal segments. This pattern is thought to conceal the larvae on the host plant (cryptic pattern) from a distance and may deter predators at close range (Fig. 1A) (*14*). It is thought that larval color pattern switching is an advanced antipredator adaptation that adjusts larval body color to the potential changes in microhabitat and foraging behavior that occur during the final instar stage (*15*).

We previously found that the larval color pattern switch in *P. xuthus* is disturbed following topical application of juvenile hormone analog (JH-analog, JHA) in the early stages of the fourth instar, yielding bird dropping–type (mimetic type) fifth instar larvae instead of the typical greenish cryptic-type larva (*16*). The effect of JHA application on the pattern switch is limited to the first 20 hours after the third molt, which is thus named the JH-sensitive period (Fig. 1B). We also found that the JH titer in the larval hemolymph declines rapidly during the JH-sensitive period. In this period, therefore, JH (the decline of the JH titer) is suggested to govern and determine the prepattern of the camouflage coloration in the final instar, although the genes and gene networks involved in its regulation remain unclarified.

Cuticle formation and pigmentation (especially melanin synthesis) for an upcoming larval instar take place mainly during the molting period, which is controlled by 20-hydroxyecdysone (20E) (*17*). Our comprehensive screening using microarray analysis has identified many genes involved in larval pigmentation or coloration during the third and fourth molts of *P. xuthus* (*18*). It is noteworthy that either pigmentation or cuticle formation, which produces the camouflage pattern that appears during the fifth instar, occurs about 3 days after prepatterning during the JH-sensitive period (Fig. 1B). Therefore, we predicted that the body color switch of *P. xuthus* larvae is composed of two separate processes: a preceding prepatterning process during the JH-sensitive period and the pigmentation process occurring during the fourth molt. However, the exact gene or gene network that reprograms the body color patterns during the JH-sensitive period remains to be elucidated.

Recent reports of the whole genome sequence of *P. xuthus*, together with associated transcriptome data (*8*, *19*), have motivated us to explore the genetic basis of the larval pattern switch. To identify the genes involved in the prepatterning process, we screened nine different RNA samples via RNA sequencing (RNA-seq) and identified 20 candidate genes that undergo spatial and temporal expression fluctuations during the JH-sensitive period. Of the candidates screened, we regarded three homeobox genes—*clawless* (hereinafter *cll*), *abdominal-A* (hereinafter *abd-A*), and *Abdominal-B* (hereinafter *Abd-B*)—as upstream transcriptional regulators. By knocking down their expression using in vivo electroporation-mediated RNA interference (RNAi) (*20*), we found that *cll* expression plays a role in eyespot marking coloration, and both *abd-A* and *Abd-B* expression play a role in the V-shaped marking pattern. In addition, the expression of all three homeobox genes was marking-specific and potentially repressed by the addition of JHA, suggesting that decreased

Department of Integrated Biosciences, University of Tokyo, Kashiwa, Japan.
*Corresponding author. Email: haruh@edu.k.u-tokyo.ac.jp

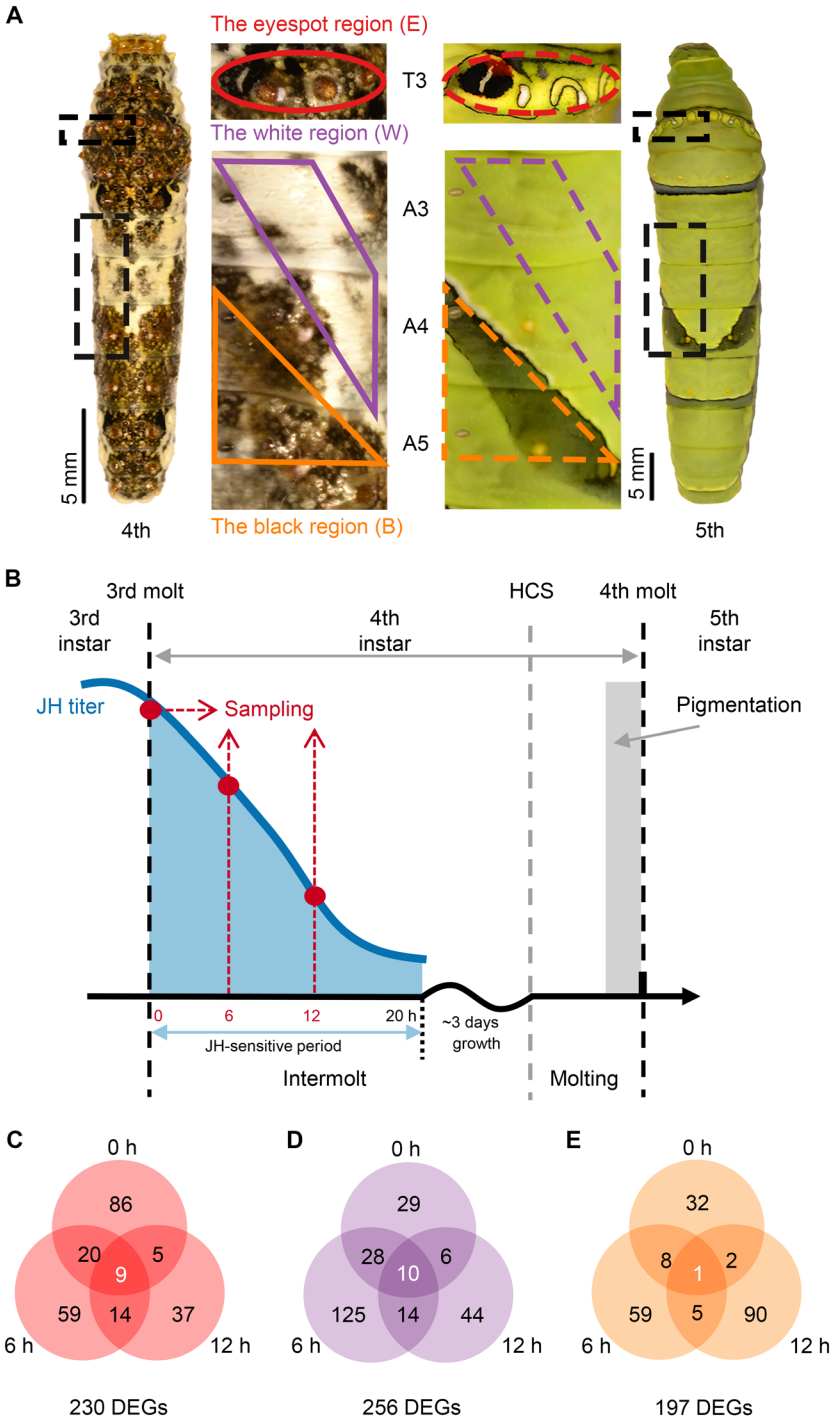

Fig. 1. Sampling strategy in RNA-seq experiment. (**A**) Body color patterns shown in the fourth and fifth instar stage. The dorsal view of the fourth instar larva (black/brown mimetic pattern) is shown on the left. The dorsal view of the fifth instar larva (green pattern) is shown on the right. The enlarged side views in the middle represent the areas where the fourth and fifth instar larvae are framed by black dashed lines, respectively. The colored lines indicate the sampling regions in the fourth instar stage. The red oval shows the eyespot region (denoted as E), the purple box shows the white region (denoted as W), and the orange box shows the black region (denoted as B). The colored dashed lines are the corresponding regions in the fifth instar after the body color switch. A3, A4, and A5: the third, fourth, and fifth abdominal segments. Scale bars, 5 mm. (**B**) Sampling time during the JH-sensitive period. The third, fourth, and fifth instars indicate the larval development stage of *P. xuthus*. The JH-sensitive period is the first 20 hours of the fourth instar. The blue line indicates the presumptive JH titer (*16*). The red dots represent the sampling time points at 0, 6, and 12 hours during the JH-sensitive period. The fourth intermolt period lasts for 2 to 3 days, and the molting period lasts for about 20 hours. The gray box indicates the pigmentation process. HCS, head capsule slippage. (**C** to **E**) DEG numbers in three sampling regions of different sampling time combinations. The central white number indicates the 20 candidate genes. Photo credit: H.J.

JH titer up-regulates the expression of these genes during the JH-sensitive period. The present study describes the early events of color patterning in larval coloration change and reveals insights into the mechanism by which hormonal regulation shapes morphological appearance in insect mimicry and camouflage.

RESULTS

Screening of color patterning–related genes based on RNA-seq data

Our previous research indicated that the larval color pattern switch in *P. xuthus* is regulated by a complex hormone-controlled gene network and that the prepatterning process during the fifth instar is likely initiated and determined during an early stage of the fourth instar, the JH-sensitive period (*16*, *18*). Although some genes for larval coloration or patterns were identified in these previous studies, the genes regulated during the JH-related period remained unidentified.

To screen the genes critical for the prepatterning or pattern switching to the fifth instar coloration, we performed RNA-seq using samples of larval epidermis from three color marking regions (Fig. 1A), at three time points during the JH-sensitive period (Fig. 1B). We selected three regions that markedly changed their colors and patterns from the fourth to the fifth instar: "the eyespot region" (hereinafter E region, on the T3 segment), "the white region" (hereinafter W region, on the third to fourth abdominal segment), and "the black region" (hereinafter B region, on the fourth to fifth abdominal segment). In the E region, the protruded structures and brown area seen during the fifth instar change to a pair of false eyespots connected by a black and green labyrinthine pattern during the fifth instar. The color of the W region changes from white to green, and the B region changes from black to green or dark green V-shaped markings (Fig. 1A). The JH-sensitive period is determined to occur from 0 to 20 hours after the third molt based on the JHA application experiment, and the JH titer in the hemolymph declines quickly during this period (*16*). Therefore, we dissected the samples at hours 0, 6, and 12 of the JH-sensitive period, each of which represents a different level of decline in the JH titer (Fig. 1B).

A total of nine RNA libraries (three epidermal regions with three sampling time points) were produced and used for the RNA-seq analyses. All RNA reads were mapped on the latest *P. xuthus* transcriptome, containing 13,102 predicted protein coding genes (*8*). To efficiently target the region-specific expressed genes that function in the prepatterning process, we used a two-step screening approach. In the first step, we compared the gene expressions in three sets of pairwise regions (fig. S1A). To screen the E-specific genes, for example, we compared the gene expressions in E versus B and in E versus W and identified those genes that were differentially expressed (fig. S1A; red spots in the left and middle columns). Thereafter, we searched the differentially expressed genes (DEGs) observed that were common to both comparisons, E versus B and E versus W (fig. S1A), and detected those genes specifically expressed in the E region (DEGs) (red spots in fig. S1B). Using this approach, we selected a total of 230 genes in the E region (fig. 1C and fig. S1B), 256 genes in the W region (Fig. 1D and fig. S1B), and 297 genes in the B region (Fig. 1E and fig. S1B). In the second step, we further compared the distribution patterns of these genes at each sampling time (Fig. 1B). On the basis of the comparison of DEGs at each sampling time, we clustered the DEGs and produced the Venn diagrams in Fig. 1 (C to E), as well as heat maps for the relative expression of region-specific DEGs in each cluster in the diagram (fig. S2). Although respective DEGs in each cluster of the Venn diagram may have important roles in prepatterning or pattern switching during the JH-sensitive period, we focused on the DEGs commonly observed across all sampling times: 0, 6, and 12 hours (Fig. 1, C to E, white numbers). According to this classification, we identified 9 genes specific to the E region (fig. S3A), 10 genes specific to the W region (fig. S3B), and 1 gene specific to the B region (fig. S3C).

Characterization of marking-specific genes expressed during the JH-sensitive period

From the 20 candidate genes screened above, 3 were characterized as homeobox genes, 2 were characterized as genes involved in cell-cell communication, 9 were characterized as putative pigmentation-related genes, 3 were characterized as cuticular protein–encoded genes, and 3 were characterized as unknown genes with low homology to any other species, which are denoted as *Papilio*-specific genes (table S1).

Transcription factors and cell communication–related genes

It is noteworthy that three of the transcription factor (TF) genes studied retain a homeobox domain. *PxGene0007795* (*Pxclawless*, *cll*) showed a high similarity to *cll* in *Drosophila melanogaster* (formerly known as *C15*) (table S1), the expression of which is necessary for leg development during the late larval stage (*21*). The RNA-seq data used for the candidate screening indicated that the expression of *cll* was observed only in the E region and increasing from 0 to 12 hours, just after the third molt (fig. S3A). *PxGene0002984* and *PxGene0002985* were classified as homologs of *abd-A* and *Abd-B*, respectively, as judged from their conserved homeobox domain sequences by phylogenetic analysis (fig. S4). *Hox* genes, *abd-A* and *Abd-B*, are members of the bithorax complex, and they play essential roles during embryogenesis (*22*). The expression of *abd-A* was observed in the B and W regions, but minimally in the E region (fig. S3A). By contrast, the expression of *Abd-B* was limited to the B region, increasing from 0 to 12 hours during the JH-sensitive period (fig. S3C). *PxGene0007446* was indicated to encode Delta, which serves as a ligand in the Notch signaling pathway (table S1), and *PxGene0011762* was indicated to encode Enhancer of split mβ [E(spl)mβ], which acts as a downstream regulator in the Notch signaling pathway (table S1) (*23*, *24*). Both genes showed a similar expression specifically in the W region during the JH-sensitive period (fig. S3B).

Pigmentation-related genes

PxGene0012461 was identified as tyrosine hydroxylase, which catalyzes tyrosine to 3,4-dihydroxyphenylalanine, the main precursors for insect melanization (table S1 and fig. S3B) (*25*), and *PxGene0001193* was identified as a homolog of the peroxidase, which is related to the neuromelanin synthesis in guinea pig brain (*26*). Both genes were similarly expressed in the E and B regions where the melanin pigments accumulate but were repressed in the W region (fig. S3B).

PxGene0003422, *PxGene0003423*, and *PxGene0003349* encode proteins containing a juvenile hormone binding protein (JHBP) domain (PfamID: PF06585). *PxGene0003422* and *PxGene0003423* were formerly annotated as putative carotenoid-binding protein 2 (PCBP2) and PCBP1, respectively (*18*). *PCBP1* was highly expressed in the E and B regions, whereas *PCBP2* was expressed only in the W region (fig. S3B). By contrast, *PxGene0003349* was specifically expressed in the E region (fig. S3A). On the basis of its temporal-specific expression and its sequence similarity with PCBP1 and PCBP2, we denoted *PxGene0003349* as the *PCBP3* gene. The other four genes were suggested to play a role in transporting the pigments or pigment precursors.

PxGene0010678 was identified as *scarlet* gene (table S1), which is involved in the transport of the red/brown pigment ommochrome (*27*). Both *PxGene0006377* and *PxGene0009224* encode the major facilitator superfamily domain (PfamID: F07690). *PxGene0006377* was predicted as *cis-muconate transporter protein* (*cts*) gene, and *PxGene0009224* was predicted as *proton-coupled folate transporter-like* gene (*PCFT-like gene*) (table S1). Both expressions were repressed in the W region but elevated in the E region (*PCFT-like gene*) or in the E and B regions (*cts*) (fig. S3, A and B). *PxGene0009442* was predicted as a putative homolog for *nose resistant to fluoxetine protein 6* (*nfr-6*) in *Caenorhabditis elegans* (table S1) (*28*), with 23% amino acid sequence similarity. The expression of this gene was dominant in the E region but was repressed gradually during the JH-sensitive period (fig. S3A).

Cuticular protein–related genes

Three genes contained domains with a low homology to the known cuticular protein group named putative cuticular protein with glycine-rich repeats and hypothetical cuticular protein hypothesis (CPH) (*29*, *30*). *PxGene0006632* (*CPH30* homolog) showed a relatively high expression in the E region (fig. S3A), and *PxGene0003756* (*CPG8* homolog) and *PxGene0003947* (*CPH16* homolog) showed a low expression in the W region (fig. S3B), indicating the possibility that these are related to the black pigmentation in the E or B region during the fifth instar.

The other three genes showed no remarkable homologs with any known genes. *PxGene0001405* (*E-selectin-like* gene) was predicted to encode a sushi repeat domain (PfamID: PF00084), which has 30% sequence identity to a brown plant hopper selectin family gene (table S1) and was repressed in the E region (fig. S3A). *PxGene0009177* was formally identified as *marking-associated unsecreted protein* (*18*), and its homolog was only found in swallowtail butterflies such as *Papilio machaon* and *Papilio polytes* (table S1). *PxGene0009177* was expressed only in the E region (fig. S3A), and this observation is also supported by the former results using in situ hybridization (*18*). *PxGene0011136* showed 28% sequence similarity with *glycine-rich cell wall structural protein 1.8-like* (XM_014501245.1) and a relatively high expression in the E region just after the third instar larva.

Temporal and spatial expressions of *cll*, *abd-A*, and *Abd-B*

Among the 20 candidate genes, many melanin-related genes and cuticular protein genes are expressed during both the third and fourth molting stages, suggesting that they are involved in both the mimetic and cryptic patterns expressed during the fourth and fifth instar, respectively (*18*, *29*). Other evidence showed that *YRG*, a downstream gene with a role in yellow pigmentation, is under trans-regulation (*18*). Thus, we reasoned that coloration genes are less likely to be involved in the prepatterning process itself. We here selected the candidate genes that were not included in the former gene list screened mainly for the pigmentation process (*18*). Therefore, we focused on three homeobox genes, *cll*, *abd-A*, and *Abd-B*, which are TFs known to regulate downstream gene networks and modify morphological characteristics (*21*, *22*).

We first checked their expressions using quantitative real-time polymerase chain reaction (qRT-PCR) under the same sampling conditions used for the RNA-seq experiment. Among the time points sampled during the JH-sensitive period, *cll* was expressed predominantly in the E region (especially at 12 hours), *Abd-B* was expressed only in the B region, and *abd-A* was expressed only in the W and B regions (Fig. 2A). These results were consistent with the expression patterns of the three genes in fig. S3 (A and C), which confirms the results of the RNA-seq analyses.

It is known that the gradient expressions of *abd-A* and *Abd-B* are essential for identity determination (*22*) of the abdominal domain of *D. melanogaster*; we thus examined their spatial expressions within the larval abdominal segments. We dissected the larval epidermis at 12 hours after the third molt and found a gradual increase in both gene expressions from segment T3 to segment A6 (head-to-tail direction), although *Abd-B* was highly expressed only in segments A5 and A6 at 12 hours after the third molt (Fig. 2B and fig. S5). To determine whether *abd-A* and *Abd-B* are related to each specific color pattern, we examined in greater detail the regional expression of both genes in the five separate abdominal regions (Fig. 2, C and D; "D," "W," "M," "V," and "G" regions; fig. S5, A and B) that show specific colors or markings at the fourth or fifth instar. Because examining these gene expressions using in situ hybridization during the JH-sensitive period in *Papilio* larvae poses a considerable technical challenge, we prepared each sample for the five regions at 12 hours after the third molt and performed qRT-PCR (Fig. 2, C and D, and fig. S5C) on each sample. The expression of *abd-A* was ubiquitous across the V-shaped marking (the V region) from segment A3 to segment A5. Unexpectedly, qRT-PCR showed that the expression of *Abd-B* was not equivalent in the B region (Fig. 1A); its expression was relatively low in the presumptive V-shaped marking (Fig. 2D, the V region), but significantly higher in the neighboring green region in segment A5 (Fig. 2D, the G region). The basal data and detailed sampling regions for Fig. 2 are shown in fig. S5.

Functional analysis: Electroporation-mediated RNAi of *cll*, *abd-A*, and *Abd-B*

To determine whether the three homeobox genes play a role in regulating the coloration pattern switch in *Papilio* larva, we next tried to knock down their gene expression during the JH-sensitive period and analyze their phenotypic effects on larval color markings. It has been suggested that RNAi is not effective in most Lepidoptera, especially in their larval stages (*31*). However, we used the electroporation-mediated RNAi method for this experiment (*20*), which enables the efficient introduction of small interfering RNA (siRNA) (negatively charged) for the target gene into the specific region (on the side of the positive electrode, hereinafter denoted as the experimental side or siRNA side) of larval epidermis via electroporation. Effects of gene knockdown can be easily observed in the introduced area (*32*, *33*). In the present study, we performed electroporation-mediated knockdown on the last day of the third instar stage and observed phenotypic effects during the fourth to fifth instar stages. We confirmed the RNAi effect using qRT-PCR and found that the expression of all three genes was significantly repressed on the experimental side at hour 12 of the JH-sensitive period (Fig. 3A).

We knocked down *cll* in the E region on the T3 segment, where we found that *cll* was highly expressed. First, we checked the RNAi effect during the fourth instar stage. However, no phenotypic changes were observed between the si-*cll* side and the control side (Fig. 3B, blue dashed oval in the fourth instar). Next, we continued to observe the RNAi effect in the fifth instar stage. The E region of the fifth instar larvae comprises a pair of false eyespots and complicated lines between them (Fig. 3B, blue dashed oval in the fifth instar).We found that the eyespot size on the si-*cll* side became smaller than that on the control side in the fifth instar (Fig. 3B and fig. S6, enlarged

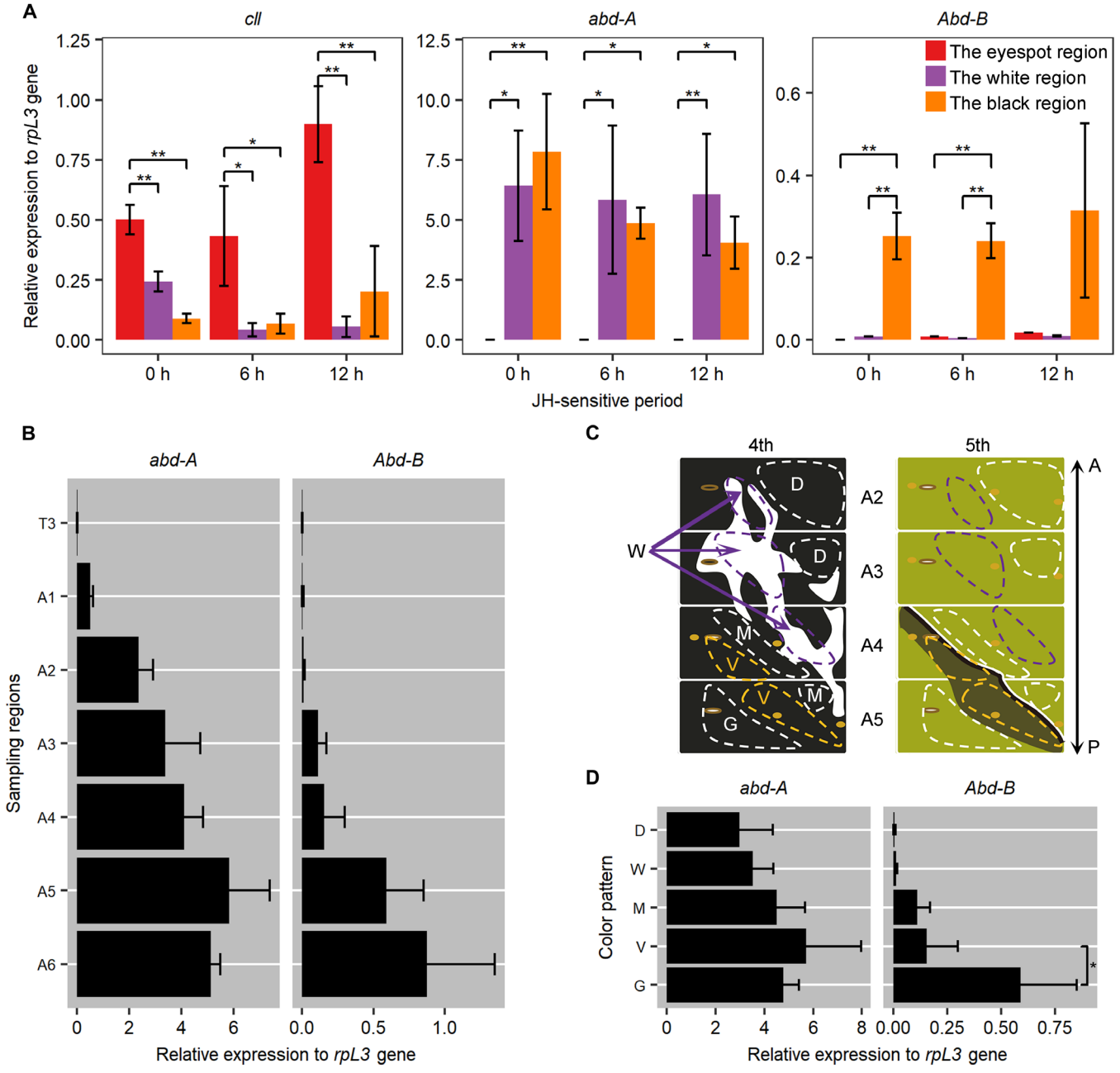

Fig. 2. Expressions of *cll*, *abd-A*, and *Abd-B* by qRT-PCR. (**A**) Relative expressions of *cll*, *abd-A*, and *Abd-B* in larval epidermis using the same sampling regions and time points as in the RNA-seq experiment. $n = 3$. Error bars indicate SD. Tukey's test, $^*P < 0.05$ and $^{**}P < 0.01$. (**B**) Relative expressions of *abd-A* and *Abd-B* in larval segments T3 to A6. The samples were dissected as shown in fig. S5. The expression of a certain gene in a particular segment was calculated as the sum of the relative expressions of that gene within that particular segment. $n = 3$. Error bars indicate SD. (**C**) The sampling regions used for detecting the precise gene expression in different color patterns. (**D**) Relative expressions of *abd-A* and *Abd-B* by presumptive fifth color patterns during the fourth instar. The expression of a certain gene in a particular color pattern was calculated as the sum of the relative expressions of that gene within that color pattern. Error bars indicate SD. Student's *t* test, $^*P = 0.0325$. *rpL3* gene was used as the inner control. D, the dorsal region that is black and lies between segments A2 and A3; W, the white region; M, the region that lies across the white region and the presumptive V-shaped marking across segments A4 and A5; G, the region that lies next to the posterior side of the presumptive V-shaped marking in segment A5; A, anterior; P, posterior.

side view, hollow blue arrowhead). In particular, the red region of the eyespot became indistinguishable in some individuals, and the complicated black lines around the eyespot appeared out of order (Fig. 3B and fig. S6, enlarged side view, blue asterisk). We further measured the size of the red area in the E region using cuticular specimen and found that the ratio of the red area significantly decreased after RNAi of *cll* (Fig. 3C). Among all the seven larvae (one in Fig. 3B and six in fig. S6) on which we performed knockdown of the *cll* gene, the pattern formation of the E regions was disturbed to varying degrees, although there were no effects on the control side (Fig. 3B and fig. S6).

Next, we knocked down the *abd-A* and *Abd-B* genes around the presumptive V-shaped marking in the B region (segments A4 to A5).

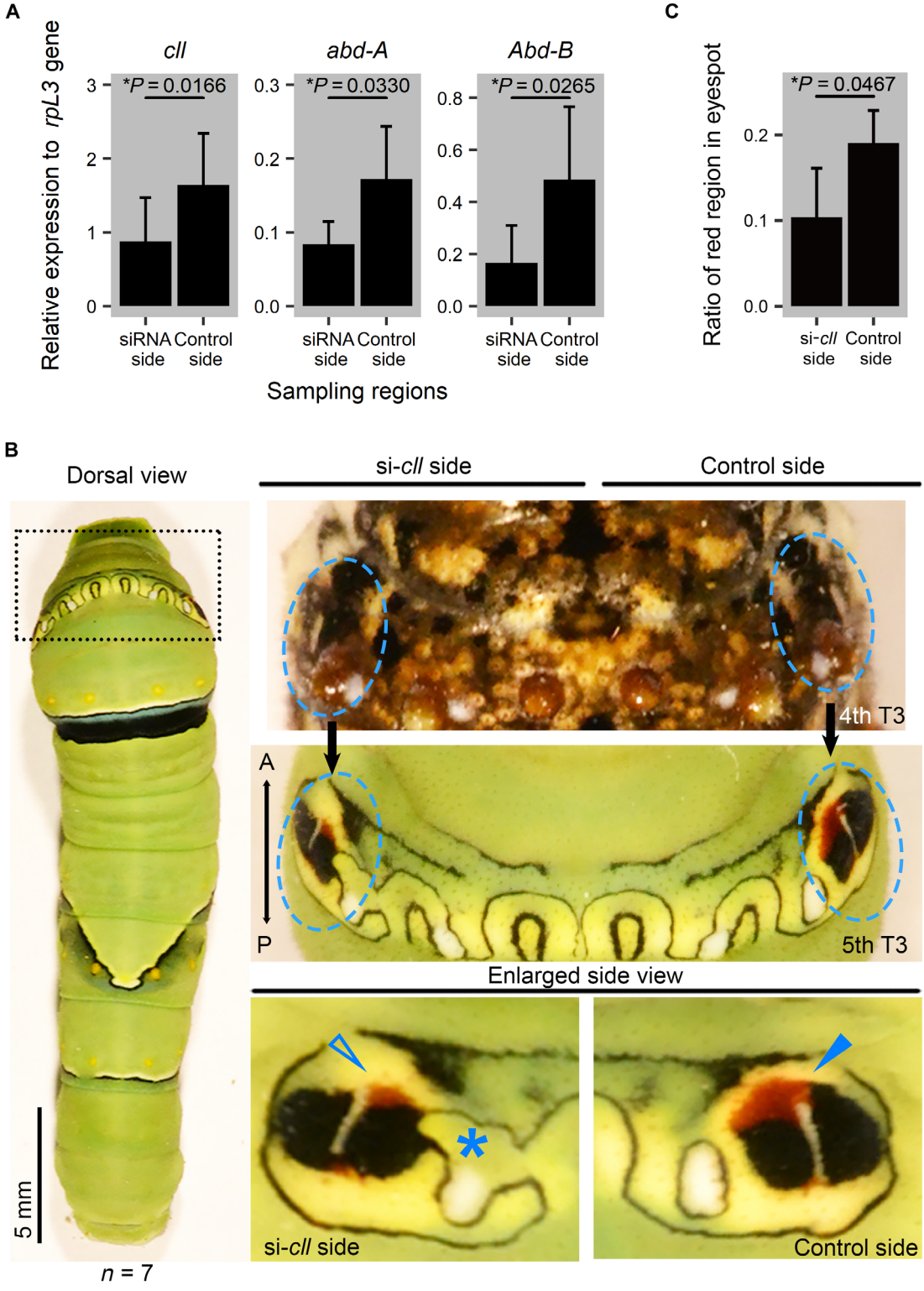

Fig. 3. Electroporation-mediated RNAi. (**A**) Measurement of knockdown effect using qRT-PCR. After injection of siRNA and electroporation, the epidermal samples were dissected at hour 12 of the fourth instar. Relative expressions of *cll* ($n = 6$), *abd-A* ($n = 5$), and *Abd-B* ($n = 5$) were measured. Student's *t* test, $^*P < 0.05$. (**B**) Injection of siRNA was performed at the end of the third instar, followed by observation during the fourth and fifth instars. Knockdown of *cll* was performed on the T3 segment (black dotted box). The blue dashed oval indicates the corresponding region of the eyespots in the fourth and fifth instars. The asterisk indicates that the complicated lines around it have changed after RNAi. The hollow arrowhead shows the si-*cll* side where the presumptive eyespot changed in size after RNAi. The filled arrowhead shows the control side where no phenotypic changes were detected. (**C**) Measurement of the red area in the E region after RNAi of *cll*. The cuticular samples were collected ($n = 3$), and the size for each region was measured using ImageJ. Student's *t* test, $^*P < 0.05$. Photo credit: H.J.

We performed RNAi at the third instar, followed by observation during the fourth and fifth instars. We confirmed that there were no phenotypic changes during the fourth instar for both RNAi of *abd-A* and *Abd-B* individuals (Fig. 4, A and B, and see the fourth phenotype in Fig. 1A). However, after *abd-A* was knocked down in the B region, the V-shaped marking in both segments A4 and A5 completely disappeared and only the green body coloration remained in the area of introduced si-*abd-A* during the fifth instar stage (Fig. 4C, enlarged side view, hollow arrowhead). In contrast, when we knocked down *Abd-B* in the B region, the V-shaped marking itself did not disappear during the fifth instar stage (fig. S7A), but some ectopic light-black regions appeared on the posterior side of the marking between segments A5 and A6 (fig. S7B).

To observe more detailed phenotypic changes during the fifth instar stage at segment A6 in which *Abd-B* was highly expressed, we further knocked down the gene at A6 and found that a larger ectopic melanized region appeared in parallel to the original two V-shaped markings on the experimental side (Fig. 4D, dashed arrowhead). Thus, the knockdown of *Abd-B* may cause an ectopic V-shaped marking between segments A5 and A6, suggesting that higher expression of *Abd-B* during the JH-sensitive period represses the formation of future V-shaped marking and causes the green coloration during the fifth instar stage.

It is noteworthy that knockdown of the above three homeobox genes during the third instar did not affect the fourth instar color patterns (Fig. 3B and Fig. 4, A and B) but broke the original pattern (*cll* or *abd-A*; Fig. 3B and Fig. 4C) or caused a new ectopic pattern (*Abd-B*) during the fifth instar stage (Fig. 4D). In addition, knockdown of *Abd-B* after the JH-sensitive period on the second or third day of the fourth instar (siRNA injection beyond the JH-sensitive period, $n = 4$; Fig. 4E) did not produce any color pattern change during the fifth instar stage. This indicates that these three genes may affect only the prepatterning process for the specific color markings of the fifth instar through their higher (or lower) region-specific expression during the JH-sensitive period. In contrast, knockdown of the *Laccase 2* (*Lac2*) gene, which plays a role in melanization during the molting period (*34*), inhibited the black/brown colorations in both the fourth and fifth instar larvae (fig. S8).

Effects of JH on prepatterning genes

Because the JH titer drastically decreased during the JH-sensitive period, most of the genes screened are thought to be regulated by the JH-signaling pathway. We applied a JHA (fenoxycarb) on the fourth instar larvae just after the third molt; prepared RNA samples from each region (E, W, and G) at 0, 6, and 12 hours after this addition; and performed RNA-seq analysis. In contrast to the expression of a known JH-inducible gene *Kr-h1* (*35*) (which is increased by the application of JH in all marking regions), those of *cll*, *abd-A*, and *Abd-B* decreased in a region-specific manner (Fig. 5A). This indicates that the expressions of three homeotic genes are repressed by JH; thus, the decreased concentration of JH in hemolymph releases gene repression.

To further explore the relationship between JH effects on prepatterning genes and the phenotypic switch, we produced the fifth instar larvae with intermediate color pattern around the T3 segment (Fig. 5B), by the addition of fenoxycarb, as described in a previous study (*16*). In these larvae, the pattern formation in the E region was disturbed in the fifth instar and the size of the red area decreased (Fig. 5B, purple arrowhead), which is similar to the phenotypic effects shown in *cll* RNAi individuals (Fig. 3B). By qRT-PCR, we confirmed a significant decrease of *cll* expression after the addition of JHA (Fig. 5C). This indicates that artificial addition of JHA inhibits the eyespot formation for the fifth instar by repressing prepatterning gene such as *cll*.

We summarized the above knockdown results of prepatterning and pigmentation genes, together with hormonal action on color pattern switching of *P. xuthus* larva in Fig. 6.

DISCUSSION

Spectacular color pattern changes are observed among caterpillars of a wide variety of *Papilio* species. In many broad-leaved plant-eating species, the bird dropping–type pattern (mimetic pattern) seen during the fourth instar stage switches to a green camouflage pattern (cryptic pattern) during the fifth instar stage, although most species in the ancestral lineage of the *Papilio* genus (subgenus *Heraclides*) show only the black and white mimetic pattern during all larval stages (*12*). It remains an open question how some *Papilio* species gain (or lose) the ability to change larval pattern during development. We predicted that the JH-mediated color pattern change may have been incorporated into larval development during *Papilio* evolution and speciation.

Using electroporation-mediated knockdown with siRNA injected during the third instar larva, we demonstrated that knockdown of the three homeobox genes caused some defects in the color patterns of the fifth instar larva, without affecting the mimetic patterns of the fourth instar larvae. This observation suggests that these genes are involved only in prepatterning of the camouflage pattern for the last larval instar, but not necessarily in all marking patterns in other stages. Many melanin-related genes and cuticular protein genes are expressed during both the third and fourth molting stages (*18*), suggesting that they are involved in both the mimetic and camouflage patterns of the fourth and fifth instars, respectively. Most of these downstream network genes, with roles in coloration or melanization, may not be involved in the prepatterning process itself. According to the prepatterns determined by upstream genes, such as the homeobox genes identified here, they are expressed during the molting stages. However, we also identified a dozen pigmentation-related or cuticular protein-related genes, the expressions of which fluctuate during the JH-sensitive period. Among them, it is presumed that the gene expressions of yellow or orange pigment-associated proteins PCB1, PCB2, and PCB3 are initiated during the JH-sensitive period, and the pigments accumulate until the greenish camouflage patterns appear during the final instar. However, the functional roles of other downstream genes expressed during the JH-sensitive period are ambiguous, and further studies are necessary to certify them.

Earlier microarray analyses of *P. xuthus* larvae revealed gene expression changes mainly during the third (making mimetic pattern) and fourth (making cryptic pattern) molting stages at six different marking regions, and many of the genes responsible for larval pattern formation or pigmentation; however, these studies did not investigate the genes regulated during the JH-sensitive period (*18*, *29*). In contrast, we have identified 20 genes with fluctuating expression patterns during the JH-sensitive period in a region-specific manner, including genes involved in transcriptional regulation [*cll*, *abd-A*, *Abd-B*, and *E(spl)mβ*] or in cell-cell communication (*delta*), which may be candidates for the JH-dependent prepatterning process. Using electroporation-mediated knockdown with siRNA, we newly confirmed that three homeobox genes function as

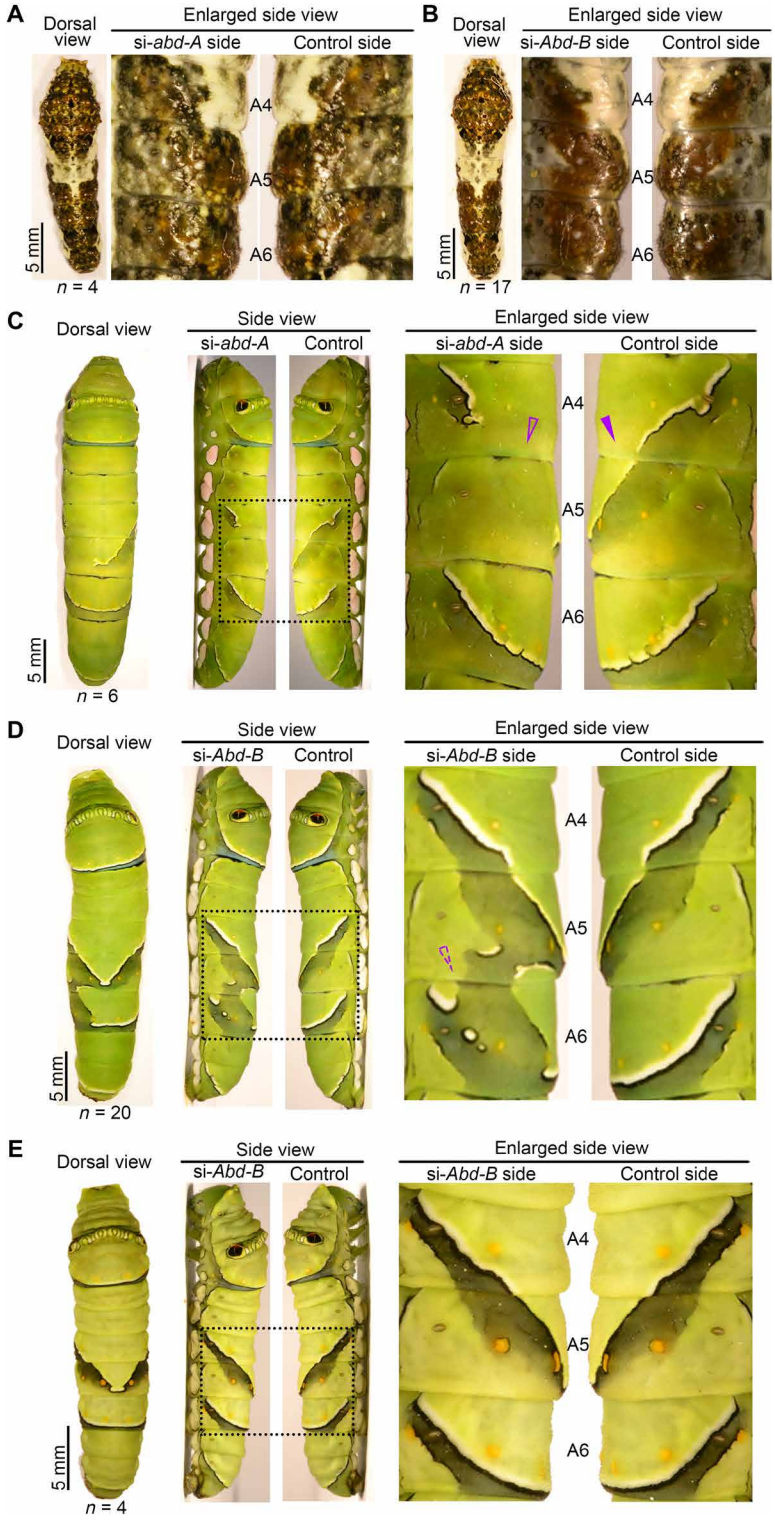

Fig. 4. Electroporation-mediated RNAi of *abd-A* and *Abd-B*. Injection of siRNA was performed at the end of the third instar, followed by observation during the fourth and fifth instars. (**A**) Phenotype of the fourth instar larva after knockdown of *abd-A* gene ($n = 4$). (**B**) Phenotype of the fourth instar larva after knockdown of *Abd-B* gene ($n = 17$). (**C**) Knockdown of *abd-A* on the segments A4 and A5. The enlarged side views show segments A4 to A6 of the experimental and control side (black dotted box). The hollow purple arrowhead indicates the regions where formation of the V-shaped marking was completely inhibited after knockdown of *abd-A*, comparing the control side indicated by a filled purple arrowhead. (**D**) Knockdown of *Abd-B* gene on segments A5 and A6 (black dotted box). The dashed purple arrowhead indicates the regions where the ectopic V-shaped marking appeared after knockdown of *Abd-B* in segment A6. (**E**) Knockdown of *Abd-B* gene after the JH-sensitive period. No phenotypic change was observed. Photo credit: H.J.

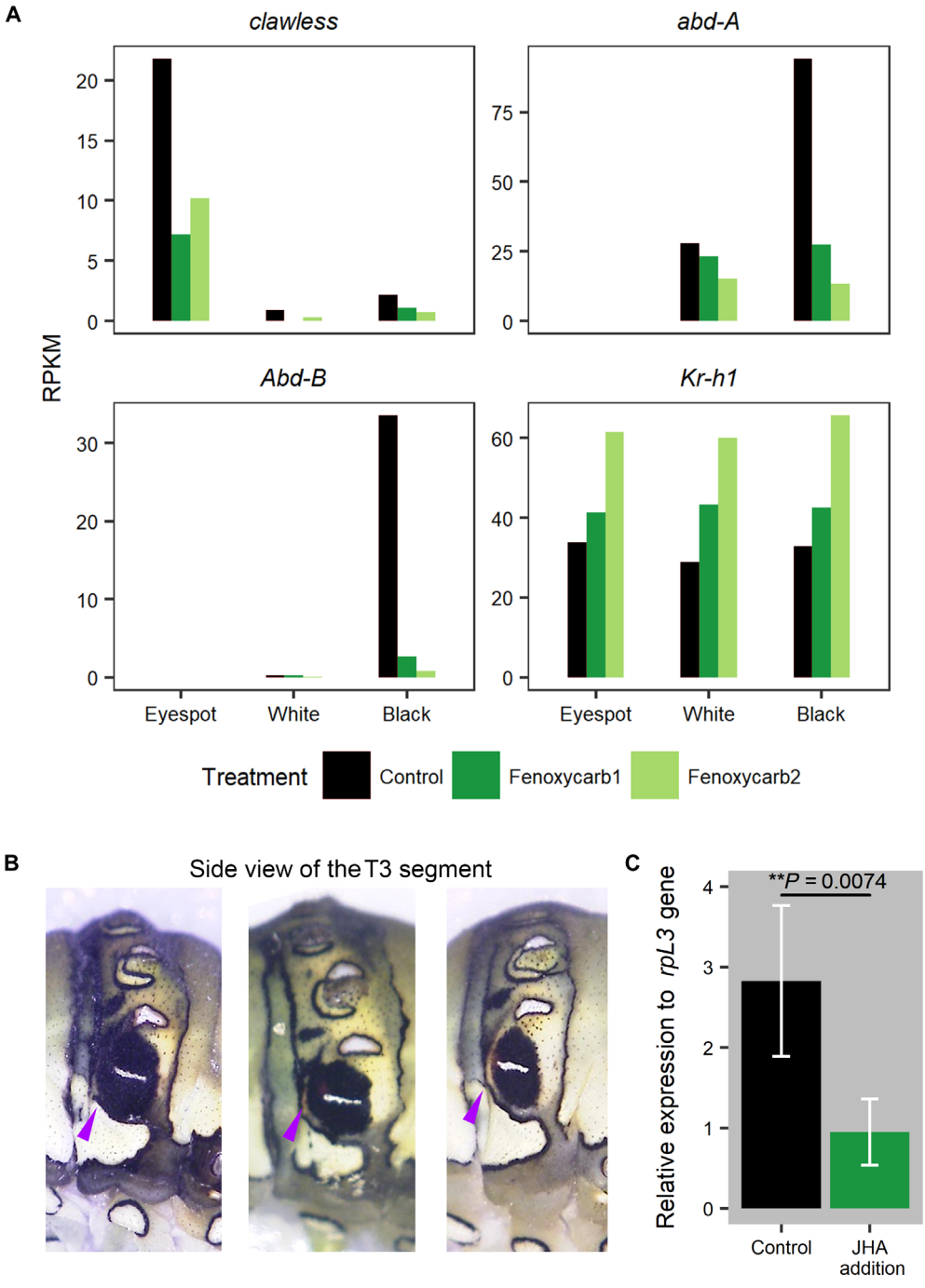

Fig. 5. Effects of JHA addition on prepatterning genes. (**A**) The expression changes of *cll*, *abd-A*, and *Abd-B* after the addition of fenoxycarb (JHA) using RNA-seq ($n = 2$, denoted as fenoxycarb1 and fenoxycarb2). The black bar indicates the control group. The green bar indicates JHA-treated samples. *Krüppel homolog 1* (*Kr-h1*) gene, a known JH response gene, was used to compare the expression before and after the addition of JHA. RPKM, reads per kilobase million. (**B**) Phenotype of the fifth instar larvae after JHA addition on the T3 segment. Fenoxycarb (5 μg per individual) was artificially applied around the T3 segment at the fourth instar stage ($n = 3$). The purple arrowhead shows the corresponding red area. (**C**) Measurement of *cll* gene expression after JHA addition using qRT-PCR. The epidermal samples around the E region were dissected at hour 12 of the fourth instar ($n = 3$). Student's *t* test, $^{**}P < 0.01$. Photo credit: T.S.

prepatterning genes for specific color markings of the cryptic pattern that develops during the fifth instar. Thus, the former and present studies revealed sets of genes that are differentially expressed at different phases: ecdysteroid-regulated genes during the molting period and JH-regulated genes during the JH-sensitive period, respectively.

Hox genes are known to define the body plan of binary animals in a spatial collinear way (along the anterior-posterior axis) (*36*). In the

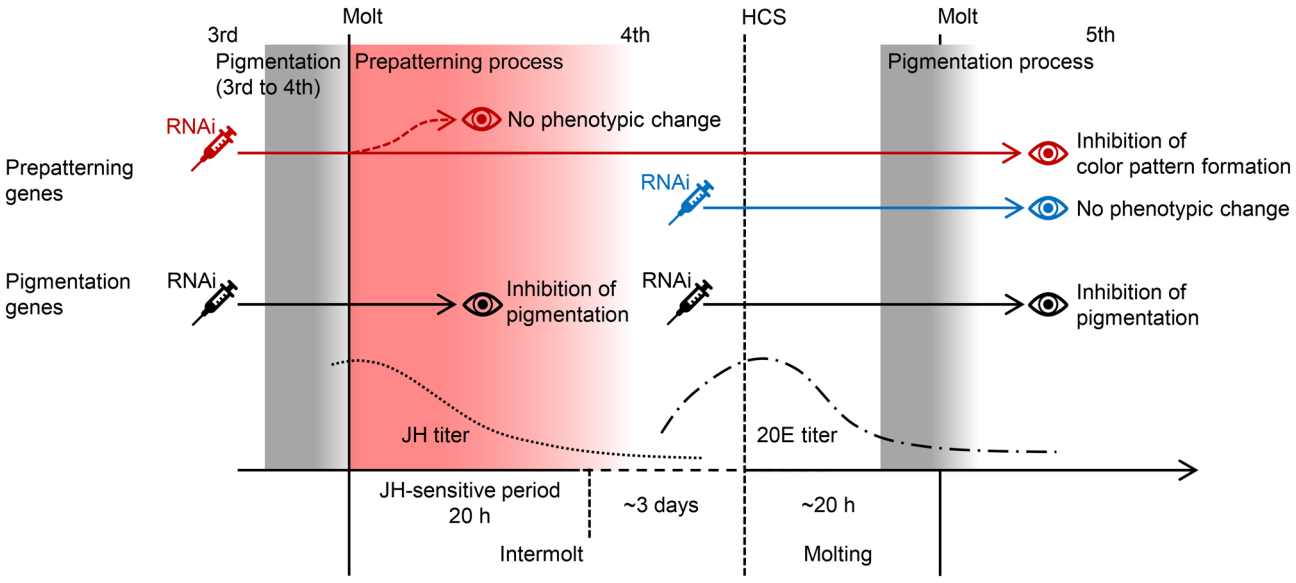

Fig. 6. A schema of color pattern switching in *P. xuthus* larva. The fourth instar larva displays bird-dropping mimetic color patterns. The fifth instar larva displays a greenish cryptic color pattern. Two processes are necessary for the body color pattern switch, and there is a 2- to 3-day developmental interval between the two processes. First, decline of the JH titer [dotted line; the JH titer is from (*16*)] in the hemolymph starts the prepatterning process in the first 20 hours of the fourth instar. During this process, spatial-specific expressions of prepatterning genes such as *cll*, *abd-A*, and *Abd-B* are detected, and RNAi of those genes inhibits normal pattern formation in the fifth but not the fourth instar (red arrow). The eye mark indicates the timing for phenotype observation. However, once the fifth color patterning is determined (at least beyond the JH-sensitive period), RNAi of prepatterning genes could not change the color patterning (blue arrow). Second, a pigmentation process occurs during the molting period as regulated by the ecdysteroid cascade [dash-dotted line; the 20E titer is from (*17*)]. RNAi of pigmentation genes, such as *Lac2*, inhibits melanization in both the fourth and fifth instars (black arrow). During this process, pigmentation genes, such as melanin synthesis–related genes, *carotenoid-binding protein* (*CBP*) genes, and *bilin-binding protein* (*BBP*) genes, are expressed in the prepatterned regions, which contribute to the visible color transition after the fourth molt.

present study, we confirmed that *abd-A* and *Abd-B* were expressed as a gradient along segments A1 to A5 and A5 to A6 in *P. xuthus* larva, respectively (Fig. 2B and fig. S5), which is in agreement with their spatial expression patterns during embryogenesis of *D. melanogaster* (*37*). Compared with our extensive knowledge of the *Hox* genes in embryogenesis, we know less about their functions and regulations in the post-embryonic stage, especially in larval development. In mammals, some *Hox* genes are expressed in the adult skeleton in regions restricted to the same expression boundaries as seen in the embryo stage and are predicted to be involved in cell regeneration during fracture repair (*38*). One possibility is that, as in expression of the *Hox* genes in mammalian skeletal tissues, the spatial expression patterns of abdA and abd-B remain consistent throughout larval development; in this case, consistent spatial expression of *abd-A* and *Abd-B* in *P. xuthus* larvae is necessary to maintain segmental identity during larval-larval molt, even after multiple rounds of cell division during repeated molting.

However, the expression of *Hox* genes is regionally dynamic during development (*37*, *39*). It is remarkable that during the fourth instar stage, and within the same segment (A5), *Abd-B* shows an expression pattern corresponding to the color pattern of the fifth instar, lower in the presumptive V-shaped marking (V) but higher in its posterior region (G) (Fig. 2D), whereas *abd-A* was ubiquitously expressed (Fig. 2D). When specifying segment identity in the fruit-fly, *abd-A* and *Abd-B* show clear expression boundaries between leads to questions regarding its potential function and regulation during the color pattern switch. The results of siRNA-based knock-down of *Abd-B* indicate that its higher expression in the posterior region (G) may repress melanin formation, causing the V-shaped marking (V) in the A5 region. There are some reports on *Hox* gene function during the formation of complex morphological traits, such as the differentiation of the "pollen basket" on the hind legs of honey bees (*40*) and cuticle formation and abdominal pigmentation in *D. melanogaster* (*37*, *41*). Although these morphological events occur mainly during metamorphosis, when the adult organs grow and develop, the body pattern switch of *P. xuthus* shown here occurs during larval development, suggesting a difference in mechanism. In the present study, we predicted that regional changes in the expression of *abd-A* and *Abd-B* occurred during the JH-sensitive period, making it possible to repattern the V-shaped marking, changing it to a different color pattern.

We also demonstrated that the knockdown of *cll* expression led to changes in the shape and size of the eyespot and its surrounding area in the T3 segment. In the E region, the red pigmented area that is known to be controlled by *ebony* (*13*, *19*) was particularly shrunken; thus, *cll* may induce *ebony* expression through the ecdysteroid-induced cascade during the fourth molting stage. We previously demonstrated that an ecdysteroid signal-related TF gene (*E75*) is expressed specifically in the E region (*18*) and is induced by the injection of 20E. In addition, another TF gene (*spalt*) is also induced during the fourth molt (but not other stages, including the third molt) specifically in the E region (*18*), suggesting that *spalt* expression is also under the control of ecdysteroid. Therefore, it is possible that *cll* determines the eyespot prepattern during the JH-sensitive period. Thereafter, according to the determined pattern, *E75* and *spalt* are induced by ecdysteroid and regulate downstream genes such as *ebony* during the fourth instar, resulting in eyespot formation. It is known that *Drosophila cll* is involved in the differentiation of the

leg distal region (*21*) and that coexpression of *cll* with *aristaless* can directly activate Notch by repressing gene expression of a Notch ligand, Delta (*42*), suggesting the possibility that the Notch signaling pathway is also involved in eyespot formation under the expression of *cll*.

The color pattern change of *P. xuthus* caterpillars is a complex developmental process that is precisely modified through multiple hormonal actions in a sequential order. On the basis of our results and earlier studies, we put forward a possible model of color pattern change in *P. xuthus* caterpillars in Fig. 6, comprising a JH-dependent prepatterning process during the JH-sensitive period and an ecdysteroid-controlled pigmentation process during the molting period. We note that, the actual transition to the fifth instar camouflage pattern occurs during the fourth molting stage, which occurs about 3 days after the JH-sensitive period (Fig. 6). Our previous JHA addition experiment and the *Abd-B* RNAi results (Fig. 4) showed that the pattern of the cryptic markings of the fifth instar should be determined during the JH-sensitive period at the beginning of the fourth instar stage and fixed thereafter, though the appearance of the fourth larval coloration remains a black/white mimetic pattern. It is not until the fourth molting period that the ecdysteroids orchestrate the pigmentation gene networks and cause the visible pattern transition following the fourth to fifth molt.

Our findings regarding the prepatterning process and three homeobox genes suggest the mechanism underlying larval color pattern change and help us understand how swallowtail butterflies protect themselves from predators during early stages of life.

MATERIALS AND METHODS

Experimental animals

P. xuthus eggs were purchased from S. Satoshi, and wild larvae were collected from a field near the Kashiwa campus of the University of Tokyo. Purchased eggs were reared on an artificial diet, and wild larvae collected from the field were reared on the leaves of *Citrus unshiu* (Rutaceae) at 25°C under long-day conditions (16 hours light and 8 hours dark). Larvae were reared in a plastic petri dish [90 mm (inner diameter) by 20 mm (height), As One Co., Osaka, Japan] for the first through the fourth instar, and the fifth instar larvae were reared in a plastic container [125 mm (inner diameter) by 100 mm (height), Mineron Kasei Co., Ltd., Osaka, Japan]. The staging of the molting period was based on the timing of the head capsule slippage.

RNA isolation and sequencing

Larvae of *P. xuthus* were first staged at the third molting period, and completion of the molt was recorded as hour 0 of the JH-sensitive period. Larvae at hours 0, 6, and 12 of the JH-sensitive period were used for sampling. Then, the larvae were anesthetized on ice and dissected in cold 1× phosphate-buffered saline. After muscle and fat body were carefully removed, the epidermis was cut according to the regions shown in Fig. 1. Total RNA was isolated using precooled TRI reagent (400 μl per sample, Sigma-Aldrich Co. LLC, Japan) and purified with deoxyribonuclease I (TaKaRa, Japan). The final RNA libraries were prepared using a TruSeq Stranded mRNA Sample Preparation Kit (Illumina) according to the manufacturer's instructions. RNA-seq was performed at the National Institute for Basic Biology of Japan using a HiSeq 2000 sequencing system (Illumina).

Gene expression and annotation

Raw reads obtained from RNA-seq were mapped to the *P. xuthus* transcriptome (Nishikawa *et al.*, PapilioBase; http://download.lepbase.org/v4/sequence/) using Bowtie 0.12.8 (*43*). The first 32 base pairs (bp) of each read were used for mapping, allowing for a mismatch of less than 2 bp. Counting data for each predicated protein coding gene were calculated. DESeq 1.30.0 (*44*) was used to test differentially expressed analysis between RNA libraries. Gene annotation was performed using online tBLASTn (E value < 1×10^{-5}) against a National Center for Biotechnology Information reference sequence database.

Phylogenetic analysis of homeobox genes

Homologs of *abd-A* and *Abd-B* in other insect species were obtained using tBLASTn (E value < 1×10^{-6}). Homologs of *cll* were obtained using BLASTx (E value < 1×10^{-6}). For *abd-A* and *Abd-B*, CDS (coding sequences, or coding regions of the genes) nucleotides were aligned using the MUSCLE method in MEGA7 (*45*) with default settings. The *Ultrabithorax* gene was used as the outer group. For *cll*, protein sequences were aligned using MUSCLE with default settings. *Distal-less-like* was used as the outer group. Gaps were removed using the pairwise deletion method. The phylogenetic tree was constructed using the neighbor-joining method in MEGA7 (*45*) and confirmed using 1000 rounds of the bootstrap test.

cDNA synthesis and qRT-PCR

For qRT-PCR, sample dissection and total RNA preparation were conducted using the same method used for RNA-seq. cDNA used for qRT-PCR was reverse-transcribed using random hexamers with a verso cDNA Synthesis Kit (Thermo Fisher Scientific Inc., USA) according to the manufacturer's instructions. qRT-PCR was performed using the StepOne Real-Time PCR System and QuantStudio 3 Real-Time PCR System (Thermo Fisher Scientific Inc., USA). The *ribosomal protein L3* (*rpL3*) gene was used as an internal control. For a single-color region, relative expression of a target gene was evaluated by (target gene expression)/(*rpL3* expression). For multiple-color regions, relative expression of a target gene was evaluated by (sum of target gene expression in regions)/(sum of *rpL3* gene expression in regions). Primers used for qRT-PCR were designed using Primer3Plus; for *abd-A*, 5′-GCGCTACCCGTGGATGTCTATC-3′ and 5′-GTGTACGTTTGTCGGCCTCGT-3′; for *Abd-B*, 5′-CGCATACGGTCTCCGGAACTA-3′ and 5′-GGTTAGAGGAGCCGCAGCCTA-3′; for *cll*, 5′-TGACAGACGCACAGGTTAAGA-3′ and 5′-GGCATGTAGCCCTTGCTTAG-3′; for *rpL3*, 5′-CTGGGCGGAGCATATGTCTGAAG-3′ and 5′-TCTTACTGGCTTTAGTGAAAGCCTTCTTC-3′; and for *Lac2*, 5′-CACAGTGTCCCATACAGCAA-3′ and 5′-ATCCTTGGAAGGTGGTTGG-3′.

Double-stranded RNA design and electroporation-mediated RNAi

Double-stranded RNAs for RNAi in *P. xuthus* larvae were designed using siDirect (version 2, http://sidirect2.rnai.jp/), and the target sequences were used as queries to search the *P. xuthus* genome to avoid off-target sites. The siRNA targeting sequences were as follows: for *cll*, 5′-GGGTTACCTTTAAATTTCTCTCA-3′; for *abd-A*, 5′-CGCAGTGAAAGAGATCAACGAGC-3′; for *Abd-B*, 5′-TACTATAATCTGCCAGTTGAAAG-3′; and for *Lac2*, 5′-ATCCTAATACCGGTTTCATGACG-3′.

For *P. xuthus* functional analysis, electroporation-mediated RNAi was performed, as previously described (*20*). Capillaries for injection were made from glass capillaries with filament (Narishige Group, Tokyo, Japan) and processed by puller-PP-830 (Narishige Group, Tokyo, Japan). A microinjector FemtoJet (Eppendorf AG, Tokyo, Japan) was used for injection. One microliter of 250 μM siRNA was injected at the intersegmental membrane between the eighth and ninth segment into the hemolymph at the third or fourth day of the third instar. Then, electroporation was performed using a NEPA21 Super Electroporator (Nepa Gene Co., Ltd., Tokyo, Japan). The parameters for electroporation were modified to avoid physical damage to larval epidermis. The poring pulse was set to 20 V lasting 5 ms, with a 50-ms interval, and was repeated twice. The transfer pulse was set to 15 V lasting 90 ms, with a 50-ms interval, and was repeated 20 times. Following electroporation, larvae were first kept in an incubator at 20°C under long-day conditions (16 hours light and 8 hours dark) for 12 hours and then subjected to normal conditions as described above. The phenotypic changes were observed and recorded during the fourth and fifth instars using a Nikon D3100. ImageJ 1.52i was used to measure the size of color marking.

Addition of JHA

P. xuthus larvae were staged from the third molting period, and fenoxycarb was applied during the JH-sensitive period. Fenoxycarb was a gift from H. Kataoka (The University of Tokyo), and it was dissolved in acetone (Wako Pure Chemical Industries, Ltd., Japan) to a final concentration of 1 μg/μl. A total of 5 μg of fenoxycarb was applied on the dorsal side of the larval integument, and 5 μl of acetone was used as a negative control. The larvae treated with fenoxycarb or acetone were reared separately.

SUPPLEMENTARY MATERIALS

Supplementary material for this article is available at http://advances.sciencemag.org/cgi/content/full/5/4/eaav7569/DC1

Fig. S1. Pairwise comparisons of gene sets among sampling regions and time points.
Fig. S2. Heat maps of DEGs in color patterns.
Fig. S3. Spatial-temporal expression of candidate genes from RNA-seq.
Fig. S4. Phylogenetic analysis of *abd-A*, *Abd-B*, and *cll*.
Fig. S5. The basal data and detailed sampling regions for qRT-PCR.
Fig. S6. Knockdown effect of *cll*.
Fig. S7. Knockdown effect of *Abd-B*.
Fig. S8. Knockdown of the pigmentation-related gene *Lac2*.
Table S1. Detailed BLASTx results of 20 candidate genes.

REFERENCES AND NOTES

1. H. W. Bates, XXXII. *Contributions to an Insect Fauna of the Amazon Valley*. LEPIDOPTERA: HELICONIDÆ. *Trans. Linn. Soc. Lond.* **23**, 495–566 (1862).
2. F. Muller, Ituna and Thyridia; a remarkable case of mimicry in butterflies. *Transactions of the Entomological Society of London* iv, (1879).
3. A. R. Wallace, *Darwinism: An Exposition of the Theory of Natural Selection, with Some of Its Applications* (Macmillan, 1889).
4. H. F. Nijhout, *The Development and Evolution of Butterfly Wing Patterns* (Smithsonian Institution, 1991).
5. J. R. True, K. A. Edwards, D. Yamamoto, S. B. Carroll, *Drosophila* wing melanin patterns form by vein-dependent elaboration of enzymatic prepatterns. *Curr. Biol.* **9**, 1382–1391 (1999).
6. M. Joron, L. Frezal, R. T. Jones, N. L. Chamberlain, S. F. Lee, C. R. Haag, A. Whibley, M. Becuwe, S. W. Baxter, L. Ferguson, P. A. Wilkinson, C. Salazar, C. Davidson, R. Clark, M. A. Quail, H. Beasley, R. Glithero, C. Lloyd, S. Sims, M. C. Jones, J. Rogers, C. D. Jiggins, R. H. ffrench-Constant, Chromosomal rearrangements maintain a polymorphic supergene controlling butterfly mimicry. *Nature* **477**, 203–206 (2011).
7. K. Kunte, W. Zhang, A. Tenger-Trolander, D. H. Palmer, A. Martin, R. D. Reed, S. P. Mullen, M. R. Kronforst, *doublesex* is a mimicry supergene. *Nature* **507**, 229–232 (2014).
8. H. Nishikawa, T. Iijima, R. Kajitani, J. Yamaguchi, T. Ando, Y. Suzuki, S. Sugano, A. Fujiyama, S. Kosugi, H. Hirakawa, S. Tabata, K. Ozaki, H. Morimoto, K. Ihara, M. Obara, H. Hori, T. Itoh, H. Fujiwara, A genetic mechanism for female-limited Batesian mimicry in *Papilio* butterfly. *Nat. Genet.* **47**, 405–409 (2015).
9. A. Mazo-Vargas, C. Concha, L. Livraghi, D. Massardo, R. W. R. Wallbank, L. Zhang, J. D. Papador, D. Martinez-Najera, C. D. Jiggins, M. R. Kronforst, C. J. Breuker, R. D. Reed, N. H. Patel, W. O. McMillan, A. Martin, Macroevolutionary shifts of *WntA* function potentiate butterfly wing-pattern diversity. *Proc. Natl. Acad. Sci. U.S.A.* **114**, 10701–10706 (2017).
10. Y. Matsuoka, A. Monteiro, Melanin pathway genes regulate color and morphology of butterfly wing scales. *Cell Rep.* **24**, 56–65 (2018).
11. S. Igarashi, *Papilionidae and Their Early Stages* (Kodansha, 1979).
12. K. L. Prudic, J. C. Oliver, F. A. H. Sperling, The signal environment is more important than diet or chemical specialization in the evolution of warning coloration. *Proc. Natl. Acad. Sci. U.S.A.* **104**, 19381–19386 (2007).
13. H. Shirataki, R. Futahashi, H. Fujiwara, Species-specific coordinated gene expression and *trans*-regulation of larval color pattern in three swallowtail butterflies. *Evol. Dev.* **12**, 305–314 (2010).
14. B. S. Tullberg, S. Merilaita, C. Wiklund, Aposematism and crypsis combined as a result of distance dependence: Functional versatility of the colour pattern in the swallowtail butterfly larva. *Proc. Biol. Sci.* **272**, 1315–1321 (2005).
15. J. K. Valkonen, O. Nokelainen, M. Jokimäki, E. Kuusinen, M. Paloranta, M. Peura, J. Mappes, From deception to frankness: Benefits of ontogenetic shift in the anti-predator strategy of alder moth *Acronicta alni* larvae. *Current Zoology* **60**, 114–122 (2014).
16. R. Futahashi, H. Fujiwara, Juvenile hormone regulates butterfly larval pattern switches. *Science* **319**, 1061 (2008).
17. R. Futahashi, H. Fujiwara, Regulation of 20-hydroxyecdysone on the larval pigmentation and the expression of melanin synthesis enzymes and *yellow* gene of the swallowtail butterfly, *Papilio xuthus*. *Insect Biochem. Mol. Biol.* **37**, 855–864 (2007).
18. R. Futahashi, H. Shirataki, T. Narita, K. Mita, H. Fujiwara, Comprehensive microarray-based analysis for stage-specific larval camouflage pattern-associated genes in the swallowtail butterfly, *Papilio xuthus*. *BMC Biol.* **10**, 46 (2012).
19. X. Li, D. Fan, W. Zhang, G. Liu, L. Zhang, L. Zhao, X. Fang, L. Chen, Y. Dong, Y. Chen, Y. Ding, R. Zhao, M. Feng, Y. Zhu, Y. Feng, X. Jiang, D. Zhu, H. Xiang, X. Feng, S. Li, J. Wang, G. Zhang, M. R. Kronforst, W. Wang, Outbred genome sequencing and CRISPR/Cas9 gene editing in butterflies. *Nat. Commun.* **6**, 8212 (2015).
20. T. Ando, H. Fujiwara, Electroporation-mediated somatic transgenesis for rapid functional analysis in insects. *Development* **140**, 454–458 (2013).
21. T. Kojima, T. Tsuji, K. Saigo, A concerted action of a paired-type homeobox gene, *aristaless*, and a homolog of *Hox11/tlx* homeobox gene, *clawless*, is essential for the distal tip development of the *Drosophila* leg. *Dev. Biol.* **279**, 434–445 (2005).
22. E. B. Lewis, A gene complex controlling segmentation in *Drosophila*. *Nature* **276**, 565–570 (1978).
23. A. M. Bailey, J. W. Posakony, Suppressor of hairless directly activates transcription of *enhancer of split* complex genes in response to Notch receptor activity. *Genes Dev.* **9**, 2609–2622 (1995).
24. S. Artavanis-Tsakonas, M. D. Rand, R. J. Lake, Notch signaling: Cell fate control and signal integration in development. *Science* **284**, 770–776 (1999).
25. R. Futahashi, H. Fujiwara, Melanin-synthesis enzymes coregulate stage-specific larval cuticular markings in the swallowtail butterfly, *Papilio xuthus*. *Dev. Genes Evol.* **215**, 519–529 (2005).
26. M. R. Okun, B. Donnellan, W. F. Lever, L. M. Edelstein, N. Or, Peroxidase-dependent oxidation of tyrosine or dopa to melanin in neurons. *Histochemie* **25**, 289–296 (1971).
27. R. G. Tearle, J. M. Belote, M. McKeown, B. S. Baker, A. J. Howells, Cloning and characterization of the *scarlet* gene of *Drosophila melanogaster*. *Genetics* **122**, 595–606 (1989).
28. R. K. M. Choy, J. H. Thomas, Fluoxetine-resistant mutants in *C. elegans* define a novel family of transmembrane proteins. *Mol. Cell* **4**, 143–152 (1999).
29. R. Futahashi, H. Fujiwara, Identification of stage-specific larval camouflage associated genes in the swallowtail butterfly, *Papilio xuthus*. *Dev. Genes Evol.* **218**, 491–504 (2008).
30. J. H. Willis, Structural cuticular proteins from arthropods: Annotation, nomenclature, and sequence characteristics in the genomics era. *Insect Biochem. Mol. Biol.* **40**, 189–204 (2010).
31. O. Terenius, A. Papanicolaou, J. S. Garbutt, I. Eleftherianos, H. Huvenne, S. Kanginakudru, M. Albrechtsen, C. An, J.-L. Aymeric, A. Barthel, P. Bebas, K. Bitra, A. Bravo, F. Chevalier, D. P. Collinge, C. M. Crava, R. A. de Maagd, B. Duvic, M. Erlandson, I. Faye, G. Felföldi, H. Fujiwara, R. Futahashi, A. S. Gandhe, H. S. Gatehouse, L. N. Gatehouse, J. M. Giebultowicz, I. Gómez, C. J. P. Grimmelikhuijzen, A. T. Groot, F. Hauser, D. G. Heckel, D. D. Hegedus, S. Hrycaj, L. Huang, J. J. Hull, K. Iatrou, M. Iga, M. R. Kanost, J. Kotwica, C. Li, J. Li, J. Liu, M. Lundmark, S. Matsumoto, M. Meyering-Vos, P. J. Millichap, A. Monteiro, N. Mrinal, T. Niimi, D. Nowara, A. Ohnishi, V. Oostra, K. Ozaki, M. Papakonstantinou, A. Popadic, M. V. Rajam, S. Saenko, R. M. Simpson, M. Soberón, M. R. Strand, S. Tomita, U. Toprak, P. Wang, C. W. Wee, S. Whyard, W. Zhang, J. Nagaraju, R. H. ffrench-Constant,

S. Herrero, K. Gordon, L. Swevers, G. Smagghe, RNA interference in Lepidoptera: An overview of successful and unsuccessful studies and implications for experimental design. *J. Insect Physiol.* **57**, 231–245 (2011).
32. J. Yamaguchi, Y. Banno, K. Mita, K. Yamamoto, T. Ando, H. Fujiwara, Periodic *Wnt1* expression in response to ecdysteroid generates twin-spot markings on caterpillars. *Nat. Commun.* **4**, 1857 (2013).
33. S. Yoda, J. Yamaguchi, K. Mita, K. Yamamoto, Y. Banno, T. Ando, T. Daimon, H. Fujiwara, The transcription factor Apontic-like controls diverse colouration pattern in caterpillars. *Nat. Commun.* **5**, 4936 (2014).
34. R. Futahashi, Y. Banno, H. Fujiwara, Caterpillar color patterns are determined by a two-phase melanin gene prepatterning process: New evidence from *tan* and *laccase2*. *Evol. Dev.* **12**, 157–167 (2010).
35. T. Kayukawa, C. Minakuchi, T. Namiki, T. Togawa, M. Yoshiyama, M. Kamimura, K. Mita, S. Imanishi, M. Kiuchi, Y. Ishikawa, T. Shinoda, Transcriptional regulation of juvenile hormone-mediated induction of Krüppel homolog 1, a repressor of insect metamorphosis. *Proc. Natl. Acad. Sci. U.S.A.* **109**, 11729–11734 (2012).
36. J. C. Pearson, D. Lemons, W. McGinnis, Modulating Hox gene functions during animal body patterning. *Nat. Rev. Genet.* **6**, 893–904 (2005).
37. N. P. Singh, R. K. Mishra, Role of *abd-A* and *Abd-B* in development of abdominal epithelia breaks posterior prevalence rule. *PLOS Genet.* **10**, e1004717 (2014).
38. D. R. Rux, D. M. Wellik, *Hox* genes in the adult skeleton: Novel functions beyond embryonic development. *Dev. Dyn.* **246**, 310–317 (2017).
39. D. Noordermeer, M. Leleu, E. Splinter, J. Rougemont, W. De Laat, D. Duboule, The dynamic architecture of Hox gene clusters. *Science* **334**, 222–225 (2011).
40. A. D. Bomtorin, A. R. Barchuk, L. M. Moda, Z. L. P. Simoes, Hox gene expression leads to differential hind leg development between honeybee castes. *PLOS ONE* **7**, e40111 (2012).
41. S. Jeong, A. Rokas, S. B. Carroll, Regulation of body pigmentation by the Abdominal-B Hox protein and its gain and loss in *Drosophila* evolution. *Cell* **125**, 1387–1399 (2006).
42. G. Campbell, Regulation of gene expression in the distal region of the *Drosophila* leg by the Hox11 homolog, C15. *Dev. Biol.* **278**, 607–618 (2005).
43. B. Langmead, C. Trapnell, M. Pop, S. L. Salzberg, Ultrafast and memory-efficient alignment of short DNA sequences to the human genome. *Genome Biol.* **10**, R25 (2009).
44. S. Anders, W. Huber, Differential expression analysis for sequence count data. *Genome Biol.* **11**, R106 (2010).
45. S. Kumar, G. Stecher, K. Tamura, MEGA7: Molecular evolutionary genetics analysis version 7.0 for bigger datasets. *Mol. Biol. Evol.* **33**, 1870–1874 (2016).

Acknowledgments: We thank S. Shimizu for providing *P. xuthus* eggs and T. Shimada and M. Kawamoto for providing citrus leaves. We also appreciate T. Kojima, R. Futahashi, Y. KonDo, S. Yoda, and T. Kitamura for helpful comments. **Funding:** This work was supported by Grants-in-Aid for Scientific Research (KAKENHI) of Japan Ministry of Education, Culture, Science and Technology (MEXT) (15H05778, 18H04880, 22128005, 20017007, 18017007, and 221S0002) to H.F. **Author contributions:** H.J. executed all of the experiments, with T.S. and J.Y. helping with sampling and analysis of RNA-seq data. H.J. and H.F. designed the experiments and wrote the paper. **Competing interests:** The authors declare that they have no competing interests. **Data and materials availability:** All data needed to evaluate the conclusions in the paper are present in the paper and/or the Supplementary Materials. Additional data related to this paper may be requested from the authors.

Submitted 17 October 2018
Accepted 14 February 2019
Published 10 April 2019
10.1126/sciadv.aav7569

Citation: H. Jin, T. Seki, J. Yamaguchi, H. Fujiwara, Prepatterning of *Papilio xuthus* caterpillar camouflage is controlled by three homeobox genes: *clawless*, *abdominal-A*, and *Abdominal-B*. *Sci. Adv.* **5**, eaav7569 (2019).